Elastoplastic Analysis of 3D Steel Frames with Semi-rigid Joints

by

Minoru SHUGYO*

A beam element for the analysis of elastoplastic large deformation of three-dimensional frames that have steel members with semi-rigid joints is presented. A plastic hinge type formulation was employed combining the 'modified incremental stiffness method', the updated Lagrangian formulation and numerical integration about the end sections of the element. The end sections of the element are discretized into small areas to estimate the plastic deformation of the element. The elastic and plastic deformations of the element are treated separately. The behavior of a semi-rigid joint is modeled as the element-end compliance. Considering the assumptions of the method, a four-element approximation for a member gives excellent results for a 3D analysis of semi-rigid and pin-connected steel frames as well as for rigid frames.The adequacy of the method is verified by comparing the results with experimental ones obtained by the author. Some examples are presented to demonstrate the accuracy and efficiency of the method.

1 INTRODUCTION

The ultimate strength and the restoring force characteristics under three-dimensional loadings are fundamental and the most important performance characteristics of a building frame. A large number of analysis methods to examine the performance of beam-columns and frames have been proposed (Al-Bermani and Kitipornchai 1990; Kouhia and Tuomala 1993; Liew et al. 1993; Hall and Challa 1995; Izzuddin and Smith 1995; Teh and Clarke 1999). Those methods can be classified into two types: the plastic zone and the plastic hinge type formulations. One of the merits of the plastic hinge type formulation is the separate treatment of elastic and plastic deformations. It means that a geometrically nonlinear stiffness can be obtained by the principle of stationary potential energy, and the 'modified incremental stiffness method' (Stricklin 1971; Washizu 1975) can be used as the numerical procedure. This is because the plastic strain energy is completely dissipated in the zero-length plastic hinges and does not affect the internal force vector of a structure. Hence, the plastic hinge type formulation can provide good accuracy as well as simplicity if the plastic deformation increment vector can be obtained precisely. In addition, the use of the plastic hinge method is suitable for frames with semi-rigid joints because a semi-rigid joint can be regarded as a kind of plastic hinge.

This paper proposes a new type of accurate beam element for the analysis of elastoplastic large deformation of three-dimensional frames that have steel members with semi-rigid joints. The element is of the plastic hinge type. The end sections of the element are discretized into small areas (fibers) to estimate the plastic deformation of the element. The elastic and plastic deformations of the element are treated separately. The elastic nonlinear tangent stiffness matrix of the element is obtained by the principle of stationary potential energy using the updated Lagrangian formulation, while the plastic deformation increments are estimated by the tangent coefficient matrix obtained by numerical integration of the hardening moduli of the fibers about the end sections.

In contrast, many other investigations concerned with semi-rigid joints have been conducted (Lui and Chen 1986; Lui and Chen 1987; Al-Bermani and Kitipornchai 1992; King and Chen 1992; King and Chen 1994; Shugyo et al. 1996; Shakourzadeh et al. 1999). It seems to the author that the node zero-length joint-element proposed by

---

* Department of Structural Engineering

Shugyo et al. (1996) and Shakourzaden et al. (1999) is the most simple and efficient method for modeling the 3D behavior of semi-rigid joints. In this paper, the tangent stiffness matrix for an element is obtained by introducing the node zero length joint-element as the element-end compliance. The 'modified incremental stiffness method' (Stricklin 1971; Washizu 1975), together with the displacement increment method (Ramm 1982), is employed as the numerical procedure.

2 ASSUMPTIONS

The following assumptions are made to form the elastoplastic tangent stiffness matrix of the element:

1) Members have thin-walled closed or open sections.

2) Cross sections remain planar and do not distort in the absence of cross-sectional warping.

3) Transverse shear deformation is negligible.

4) Deflection is large but elastic strain is small.

5) Axial stress and the shear stress due to St. Venant torsion participate in the yielding of the fibers of members with closed sections, while only axial stress participates for the members with open sections.

6) Plastic deformation consists of only four components that correspond to axial force, biaxial bending moments, and torsional moment or bimoment.

7) There is no local buckling.

8) Although actual generalized plastic strain in a short element is generally distributed nonlinearly (Fig. 1(a)), the distribution is assumed to be linear with the values at element nodes i and j (Fig. 1(b)).

9) Incremental plastic deformations in the two $l/2$ portions occur concentrically in the plastic hinge of zero length at element nodes i and j, where l is the length of the element.
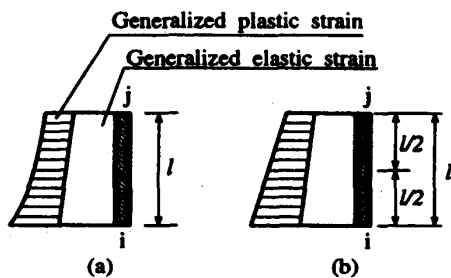

Fig.1 Assumption of generalized plastic strain distiribution in an element

3 GEOMETRICALLY NONLINEAR STIFFNESS MATRIX

The initial element coordinate systems (x,y,z) and $(\bar{x},\bar{y},\bar{z})$ are shown in Fig. 2 for an element of a general open section. The x-axis is perpendicular to the cross section and passes through the centroid O of the end cross section; the y- and z- axes are the principal axes of the cross section at node i. A parallel set of axes $\bar{x},\bar{y},\bar{z}$ pass through the shear center S of the cross section at node i. The strain-displacement relationship adopted here is
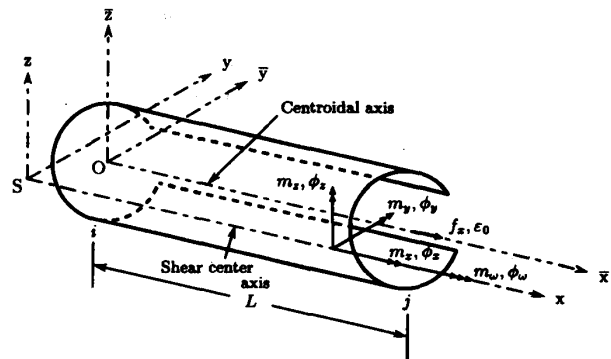

Fig.2 Element coodinate system and components of generalized stress and strain

$$
\left.
\begin{aligned}
\epsilon_x &= \frac{\partial u}{\partial x} + \frac{1}{2}\left(\frac{\partial v}{\partial x}\right)^2 + \frac{1}{2}\left(\frac{\partial w}{\partial x}\right)^2 \\
\gamma_{xy} &= \frac{\partial v}{\partial x} + \frac{\partial u}{\partial y} \\
\gamma_{xz} &= \frac{\partial w}{\partial x} + \frac{\partial u}{\partial z} \\
\epsilon_y &= \epsilon_z = \gamma_{yz} = 0
\end{aligned}
\right\}
\tag{1}
$$

where u, v, and w are the displacements of an arbitrary point in x-, y-, and z-direction, respectively. These values are related to the displacements u_0 of the point on the x-axis, v_0, and w_0, and the rotation angle ψ_0 of the point on the $\bar{x}$ axis as

$$
\left.
\begin{aligned}
u &= u_0 - y\frac{dv_0}{dx} - z\frac{dw_0}{dx} + \omega_s\frac{d\psi_0}{dx} \\
v &= v_0 - \bar{z}\psi_0 \\
w &= w_0 + \bar{y}\psi_0
\end{aligned}
\right\}
\tag{2}
$$

where ω_s is the normalized warping function about the shear center. Substituting (2) into (1) and utilizing the 'modified incremental stiffness method' (Stricklin 1971; Washizu 1975), we obtain the following equation:

$$
dQ + R = K^e dq^e
\tag{3}
$$

in which K^e is the geometrically nonlinear tangent stiffness matrix, R is the out-of-balance force vector and Q and q^e

are the nodal force vector and the nodal elastic displacement vector of an element, respectively. Q and q^e have the following components:

$$
\begin{aligned}
Q = [F_{xi} \quad F_{yi} \quad F_{zi} \quad M_{xi} \quad M_{yi} \quad M_{zi} \quad M_{\omega i} \\
F_{xj} \quad F_{yj} \quad F_{zj} \quad M_{xj} \quad M_{yj} \quad M_{zj} \quad M_{\omega j}]^T \\
q^e = [u_i^e \quad v_i^e \quad w_i^e \quad \theta_{xi}^e \quad \theta_{yi}^e \quad \theta_{zi}^e \quad \theta_{zi}'^e \\
u_j^e \quad v_j^e \quad w_j^e \quad \theta_{xj}^e \quad \theta_{yj}^e \quad \theta_{zj}^e \quad \theta_{zj}'^e]^T
\end{aligned}
\qquad (4)
$$

where F_{kl} denotes the force in the k- direction at node l ; M_{kl} denotes the bending or torsional moment about the k- axis at node l ; and $M_{\omega l}$ denotes the bimoment at node l. Components of q^e are the corresponding elastic displacements. The rotation matrix for large rotation (Crisfield 1997) was used to determine the successive element coordinate system and the nodal total local displacements. Therefore, some components of the total nodal local displacements that are contained in K^e at the last known state (reference configuration) are as follows if the element is in the elastic range: $u_i^e = v_i^e = w_i^e = v_j^e = w_j^e = 0$ and $\theta_{xi}^e = -\theta_{xj}^e$. Cubic functions for v_0, w_0 and ψ_0 and linear function for u_0 are adopted as displacement fields.

4 ESTIMATION OF PLASTIC DEFORMATION INCREMENTS

In the present formulation, a plastic deformation increment of an element is estimated utilizing a tangent coefficient matrix for a cross section. The tangent coefficient matrix is obtained by numerical integration of the tangent stiffnesses of the fibers that compose the element.

4.1 Incremental Stress-Strain Relationship of a Fiber

For a member with a thin-walled closed section, using the von Mises yield condition, associated flow rule, and Ziegler's hardening rule, we can obtain the following equation (Armen et al. 1970; Shugyo et al. 1995) from assumption (5):

$$
\left\{ \begin{array}{c} d\sigma \\ d\tau \end{array} \right\} = \left[\begin{array}{cc} D_{11} & D_{12} \\ D_{21} & D_{22} \end{array} \right] \left\{ \begin{array}{c} d\epsilon \\ d\gamma \end{array} \right\} \equiv D^p \left\{ \begin{array}{c} d\epsilon \\ d\gamma \end{array} \right\}
\qquad (5)
$$

where σ is a normal stress due to axial force and bending moments, τ is a shear stress due to St. Venant torsion.

For a member with a thin-walled open section, the incremental stress-strain relationship of a fiber is expressed as:

$$
d\sigma = E_t d\epsilon
\qquad (6)
$$

where σ is a normal stress due to axial force, bending moments, and bimoment, and E_t is the tangent modulus of the uniaxial stress-strain relationship of a fiber.

4.2 Plastic Tangent Coefficient Matrix for a Section
4.2.1 Thin-walled Closed Section

The components of the generalized stress vector and generalized strain vector are shown in Fig. 2. From assumptions (5) and (6), the components of the generalized stress vector f_c and generalized strain vector δ_c for a thin-walled closed section can be written as:

$$
\begin{aligned}
f_c = [f_x \quad m_x \quad m_y \quad m_z]^T \\
\delta_c = [\epsilon_0 \quad \phi_x \quad \phi_y \quad \phi_z]^T
\end{aligned}
\qquad (7)
$$

where f_x is an axial force, m_x is a torsional moment, m_y and m_z are bending moments. The components of δ_c are corresponding generalized strains. The increments of the generalized stresses are related to the fiber stress increments by

$$
\begin{aligned}
df_x = \int d\sigma dA \qquad dm_x = \int d\tau h dA \\
dm_y = \int d\sigma z dA \qquad dm_z = -\int d\sigma y dA
\end{aligned}
\qquad (8)
$$

whereas the fiber strain increments are related to the increments of the generalized strains by

$$
\begin{aligned}
d\epsilon = d\epsilon_0 + z d\phi_y - y d\phi_z \\
d\gamma = h d\phi_x
\end{aligned}
\qquad (9)
$$

where h is a section constant. If the wall thickness of a tube is constant, $h = r$ for a circular hollow section and $h = ab/(a+b)$ for a rectangular hollow section where r is the mean radius, a is the mean width, and b is the mean depth of the section (Teh and Clarke 1999).Substituting (5) and (9) into (8), we obtain the incremental generalized stress-generalized strain relationship:

$$
df_c = \left[\begin{array}{cccc} \int D_{11} dA & \int D_{12} h dA & \int D_{11} z dA & -\int D_{11} y dA \\ \int D_{21} h dA & \int D_{22} h^2 dA & \int D_{21} h z dA & -\int D_{21} h y dA \\ \int D_{11} z dA & \int D_{12} h z dA & \int D_{11} z^2 dA & -\int D_{11} y z dA \\ -\int D_{11} y dA & -\int D_{12} h y dA & -\int D_{11} y z dA & \int D_{11} y^2 dA \end{array} \right] d\delta_c \equiv s d\delta_c
\qquad (10)
$$

where s is a tangent coefficient matrix. Let s^e denote an elastic tangent coefficient matrix and let $d\delta_c^e$ and $d\delta_c^p$ denote the elastic and plastic components of $d\delta_c$, respectively, then

$$
\begin{aligned}
df_c = s^e d\delta_c^e \\
d\delta_c = d\delta_c^e + d\delta_c^p
\end{aligned}
\qquad (11)
$$

Substituting (10) into (11) yields

$$d\delta_e{}^p = (s^{-1} - s^{e^{-1}})df_c \equiv s'df_c \tag{12}$$

where s' is a plastic tangent coefficient matrix. The elastic tangent coefficient matrix s^e is constant for any state of the section.

4.2.2 Thin-walled Open Section

We can obtain the plastic tangent coefficient matrix s' for an open section in the same way as described above using (6) instead of (5) (Chen and Atsuta 1977).The components of generalized stress vector f_o and generalized strain vector δ_o for a thin-walled open section are:

$$\left. \begin{aligned} f_o &= [f_x \quad m_y \quad m_z \quad m_\omega]^T \\ \delta_o &= [\epsilon_0 \quad \phi_y \quad \phi_z \quad \phi_\omega]^T \end{aligned} \right\} \tag{13}$$

where m_ω is a bimoment and ϕ_ω is the corresponding generalized strain.

For both closed and open sections the components of the tangent coefficient matrix can be obtained by numerical integration. Figure 3 shows the partitioning of a cross section used in the analyses described later. The stress and the tangent stiffness in each fiber are obtained as the average values at its centroid. The 'tangent stiffness method' (Chen and Atsuta 1977) can be used to determine the matrix s.
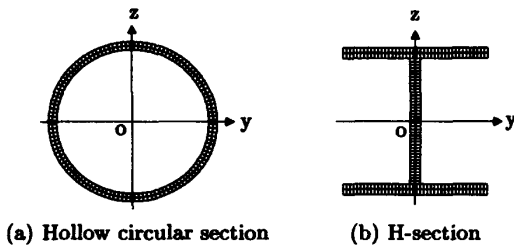

(a) Hollow circular section   (b) H-section

Fig.3 Partitioning of a cross section

4.3 Estimation of Plastic Deformation Increments

Now, let us define the plastic deformation increments in the plastic hinges $dq_i{}^p$ and $dq_j{}^p$ as

$$\left. \begin{aligned} dq_i{}^p &= [du_i^p \quad 0 \quad 0 \quad d\theta_{xi}^p \quad d\theta_{yi}^p \quad d\theta_{zi}^p \quad 0]^T \\ dq_j{}^p &= [du_j^p \quad 0 \quad 0 \quad d\theta_{xj}^p \quad d\theta_{yj}^p \quad d\theta_{zj}^p \quad 0]^T \end{aligned} \right\} \tag{14}$$

for an element with a thin-walled closed section and

$$\left. \begin{aligned} dq_i^p &= [du_i^p \quad 0 \quad 0 \quad d\theta_{yi}^p \quad d\theta_{xi}^p \quad d\theta_{zi}'^p]^T \\ dq_j^p &= [du_j^p \quad 0 \quad 0 \quad d\theta_{yj}^p \quad d\theta_{zj}^p \quad d\theta_{zj}'^p]^T \end{aligned} \right\} \tag{15}$$

for an element with a thin-walled open section, which are the deformation increments due to the generalized plastic strain increments of an element. These plastic deformation increments can be obtained as described below.

The generalized stresses at the element ends are obtained by the nodal forces at the last known state with their coordinate transformation. (Note that the i-node cross section is the negative plane about the x- and $\bar{x}$ axes.) Using these generalized stresses, we can obtain the plastic tangent coefficient matrices s_i' and s_j' utilizing the procedure explained above. Representing the components of s_i' by $(s_{kl}')_i$, a new square matrix s_i^p of the 7th order can be obtained as follows:

$$s_i^p = \begin{bmatrix} (s_{11}')_i & 0 & 0 & (s_{12}')_i & (s_{13}')_i & (s_{14}')_i & 0 \\ 0 & 0 & 0 & 0 & 0 & 0 & 0 \\ 0 & 0 & 0 & 0 & 0 & 0 & 0 \\ (s_{21}')_i & 0 & 0 & (s_{22}')_i & (s_{23}')_i & (s_{24}')_i & 0 \\ (s_{31}')_i & 0 & 0 & (s_{32}')_i & (s_{33}')_i & (s_{34}')_i & 0 \\ (s_{41}')_i & 0 & 0 & (s_{42}')_i & (s_{43}')_i & (s_{44}')_i & 0 \\ 0 & 0 & 0 & 0 & 0 & 0 & 0 \end{bmatrix} \tag{16}$$

for a closed section element and

$$s_i^p = \begin{bmatrix} (s_{11}')_i & 0 & 0 & (s_{12}')_i & (s_{13}')_i & (s_{14}')_i \\ 0 & 0 & 0 & 0 & 0 & 0 \\ 0 & 0 & 0 & 0 & 0 & 0 \\ 0 & 0 & 0 & 0 & 0 & 0 \\ (s_{21}')_i & 0 & 0 & (s_{22}')_i & (s_{23}')_i & (s_{24}')_i \\ (s_{31}')_i & 0 & 0 & (s_{32}')_i & (s_{33}')_i & (s_{34}')_i \\ (s_{41}')_i & 0 & 0 & (s_{42}')_i & (s_{43}')_i & (s_{44}')_i \end{bmatrix} \tag{17}$$

for an open section element. Another new matrix s_j^p that corresponds to s_j' can be similarly obtained. In the case of uniaxial bending, the plastic curvature increment is distributed as shown in Fig. 4 from assumption (8). Hence the plastic rotation increment at the element end i can be expressed as follows using a trapezoidal rule from assumption (9):

$$-d\theta_{yi}^p = \frac{1}{2} \cdot \frac{l}{2} \left\{ d\phi_{yi}^p + \frac{1}{2}(d\phi_{yi}^p + d\phi_{yj}^p) \right\} = \frac{l}{2} \cdot \frac{3d\phi_{yi}^p + d\phi_{yj}^p}{4}. \tag{18}$$
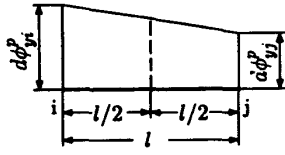
Fig. 4 Assumed plastic curvature distribution in an element

The plastic deformation increments at the element end i can be obtained by extending (18) considering that the i-node section is a negative plane and expressed as

$$dq_i^p = \frac{l}{2} \cdot \frac{3s_i^p dQ_i - s_j^p dQ_j}{4}. \qquad (19)$$

Similarly, for the element end j

$$dq_j^p = \frac{l}{2} \cdot \frac{-s_i^p dQ_i + 3s_j^p dQ_j}{4}. \qquad (20)$$

Rearranging (19) and (20), we obtain

$$\left\{ \begin{array}{c} dq_i^p \\ dq_j^p \end{array} \right\} = \frac{l}{8} \left[\begin{array}{cc} 3s_i^p & -s_j^p \\ -s_i^p & 3s_j^p \end{array} \right] \left\{ \begin{array}{c} dQ_i \\ dQ_j \end{array} \right\} \equiv s^p dQ. \qquad (21)$$

5 DEFORMATION INCREMENTS IN SEMI-RIGID JOINTS

The matrix s^p in (21) is a compliance matrix that relates the nodal plastic deformation increment vector to the nodal force increment vector. Almost the same expression can be written for the deformation increment vector in a semi-rigid joint at node i if the interaction effects are negligible (Shugyo et al. 1996, Shakourzaden et al. 1999) as follows:

$$dq_i^s = \begin{bmatrix} 0 & 0 & 0 & 0 & 0 & 0 & 0 \\ 0 & 0 & 0 & 0 & 0 & 0 & 0 \\ 0 & 0 & 0 & 0 & 0 & 0 & 0 \\ 0 & 0 & 0 & (c_{44})_i & 0 & 0 & 0 \\ 0 & 0 & 0 & 0 & (c_{55})_i & 0 & 0 \\ 0 & 0 & 0 & 0 & 0 & (c_{66})_i & 0 \\ 0 & 0 & 0 & 0 & 0 & 0 & (c_{77})_i \end{bmatrix} dQ_i \equiv c_i dQ_i. \quad (22)$$

where dq_i^s is the deformation increment vector in the zero length semi-rigid element at nodes i. Similarly, we can obtain the matrix c_j for node j and hence

$$dq^s = c dQ \qquad (23)$$

6 ELASTOPLASTIC TANGENT STIFFNESS MATRIX

Assuming that the total displacement increment dq is the sum of the elastic displacement increment dq^e, the plastic deformation increment dq^p, and the deformation increment in the zero length semi-rigid elements dq^s we obtain

$$dq^e = dq - dq^p - dq^s. \qquad (24)$$

From (3) the linearized relationship between dQ and dq^e is given as $dQ = K^e dq^e$, hence

$$dQ = K^e dq - K^e (dq^p + dq^s). \qquad (25)$$

Substituting (21) and (23)into (25), we obtain

$$dQ = K^e dq - K^e (s^p + c) dQ. \qquad (26)$$

Rearranging (26) and again introducing the concept of 'modified incremental stiffness method', we can obtain the following equation:

$$dQ + R = [I + K^e (s^p + c)]^{-1} K^e dq \equiv K^p dq \qquad (27)$$

where I is the unit matrix, R is the out-of-balance force vector,and K^p is the elastoplastic tangent stiffness matrix. Numerical analysis can be conducted by Ramm's displacement increment method (Ramm 1982) using (27).The coordinate transformation matrix of an element is updated, and the total nodal local displacements are recomputed by separating the rigid body displacements in each step by using the rotation matrix. R is obtained by the explicit expressions using the elastic total nodal local displacements, which can be obtained by subtracting the sum of the plastic deformation increments and the deformation increments in the semi-rigid elements from the total nodal local displacements.

The use of the 'modified incremental stiffness method' may cause a significant error if the size of the displacement increment is not appropriate. Therefore, the author used the following procedure to determine the size of the displacement increment. (1)Examine the magnitude of the generalized strain increments in the last step for all elements and obtain the maximum value. (2)Determine the size of the displacement increment of the next step using the sizes of the displacement increment and maximum

generalized strain increment in the last step so that the maximum value of the generalized strain increment in the next step is less than the prescribed standard value. As the standard value for all the following examples, the author used a value of 0.01, which is the nondimensionalized value determined by the initial yield value of each element.

7 NUMERICAL EXAMPLES

7.1 Cantilever Beams subjected to Shear Force and Torsional Moment

The adequacy of the present method on determining the bending-torsional behavior of a beam is examined by comparing the results with experimental results of cantilever beams subjected to shear force and torsional moment. Figure 5 shows the test arrangement. The test specimens were two steel beams, one with a hollow circular section and one with an H-section. Both specimens were annealed at 630 degrees Celsius for one hour. The sizes and mechanical properties of the specimens are as follows: outside diameter of the cross section D_c =10.17 cm, thickness t_c =0.41 cm, length L_t =55.30 cm, Young's modulus E_c =207.8 GPa, yield stress σ_{yc} =299.9 MPa for the beam with the hollow circular section, and width of the section W_h =10.10 cm, depth D_h =10.00 cm, flange thickness t_f =0.77 cm, web thickness t_w =0.57 cm,length L_t =51.40 cm, Young's modulus E_h =205.8 GPa, yield stress σ_{yh} =271.5 MPa for the beam with the H-section.
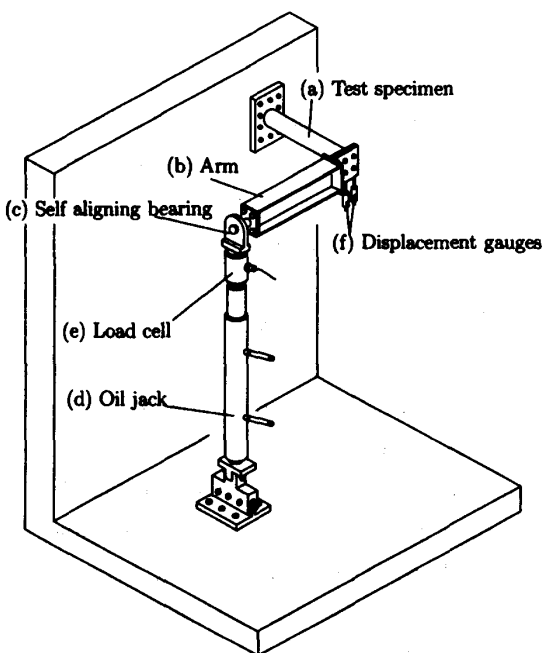

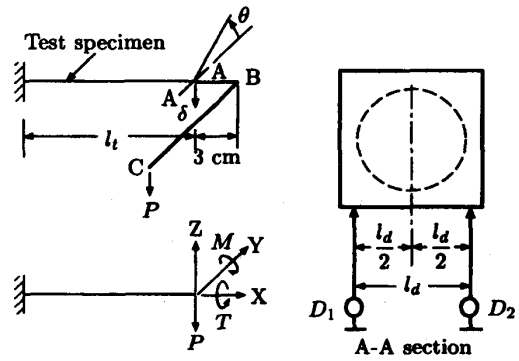Fig. 5 Test arrangement for cantilever beam

Fig. 6 Scheme of loading and measuring system

Figure 6 shows the scheme of loading and the measuring system. The distance from point B to point C in the figure is 73.0 cm. The load P causes the shear force P, the bending moment M, and the torsional moment T at the top of the test specimen (A-A section), where M =3P and T=73cos θP. The H-beam was set so the weak axis of the cross section was aligned with the direction of the shear force. The warping of both end sections was restrained by end plates 3.0 cm thick. The vertical deflection δ and torsional angle θ can be obtained from the outputs of two displacement gauges δ_1 and δ_2 as follows:

$$\left. \begin{array}{l} \delta = (\delta_1 + \delta_2)/2 \\ \theta = \tan^{-1}((\delta_2 - \delta_1)/l_d) \end{array} \right\} \qquad (28)$$

In the numerical analyses, the elastic shear moduli $G_c = E_c/2.6$, $G_h = E_h/2.6$ and strain hardening moduli in the elastoplastic range $H_c = E_c/100$, $H_h = E_h/100$ were assumed in addition to the above-mentioned material constants. Considering assumption (8) of the method, the beam was divided into two elements by the node at a point 1/5 of the beam length. The relationships of load versus vertical deflection and load versus torsional angle at the beam top are shown in Figs. 7 and 8. Although some errors are present, the figures show that this method gives an accurate result for a beam member.
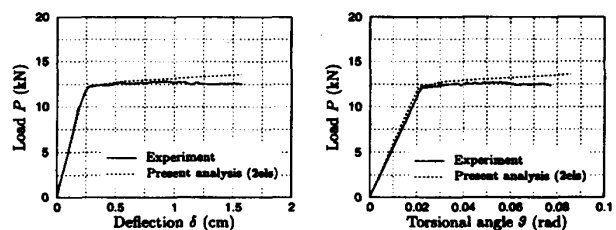

Fig. 7 Load-deflection and load-torsional angle relationships at the beam top (hollow circular section)
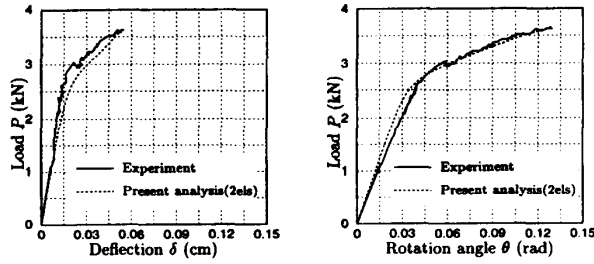
Fig. 8 Load-deflection and load-torsional angle
relationships at the beam top (H-section)

7.2 Three-Dimensional Frame

The adequacy of the present method on the elastoplastic
behavior of a 3D frame is examined by using the equilateral
triangular space frame tested and analyzed by Harrison
(1964) and Teh and Clarke (1999) (Fig. 9). The properties
of the members are given in the figure. In the present
analysis, each member was modeled in the same manner as
Teh and Clarke, that is, each column was modeled with
four equal-length elements, while the beams were modeled
with two or six equal-length elements depending on the
loading condition. Strain hardening modulus H=E/100 was
assumed, whereas Teh and Clarke assumed H=0.

$V = 1.3H$

All members CHS
$L = 48$ in
$D = 1.682$ in
$t = 0.176$ in
$E = 28800$ ksi
$G = 11520$ ksi

Columns: $\sigma_y = 30.6$ ksi
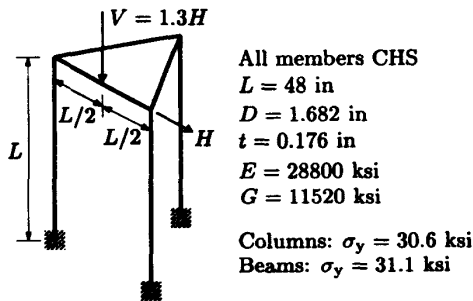Beams: $\sigma_y = 31.1$ ksi

Fig. 9 Harrison's (1964) space frame

Figure 10 compares the relationship between the
horizontal load and the horizontal sway of the right eave.
The result of the present method agrees with the numerical
results of Teh and Clarke in the elastic range; the restoring
force in the elastoplastic range is slightly small in
comparison with the other two results. The increase in the
number of elements narrows the discrepancy between the
two results of Harrison and the present method. As is
obvious from assumption (8), the use of this method with
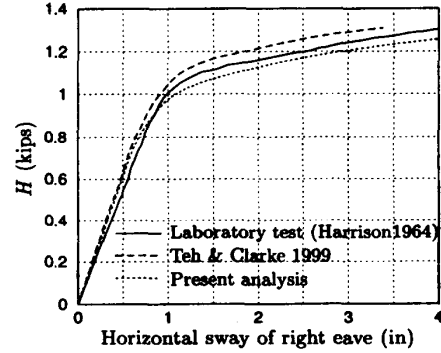fewer modeling elements gives a solution that is more
conservative.

Fig. 10 Load-displacement curves for Harrison's (1964)
space frame

7.3 Semi-rigid Rectangular Frame

Liew et al. (1997) carried out a series of tests on a variety
of semi-rigid rectangular frames. The test frames can be
used for a calibration of analysis method. Figure 11 shows
the dimensions of the SRF1 frame. The sizes and
mechanical properties of the columns and the beam are as
follows: depth D=22.23 cm, width B=20.88 cm, flange
thickness t_f =2.05 cm, web thickness t_w =1.30 cm, yield
stress σ_y =318.0 MPa for the columns, and D=35.86 cm,
B=17.21 cm, t_f=1.30 cm, t_w=0.80 cm, σ_y =303.0 MPa for the
beam. The moment-rotation relationships for the beam-to-
column connection and for the column base obtained by the
tests are shown in Figs. 12 and 13. The dotted lines in the
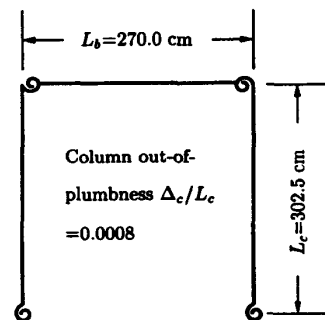figures are approximate curves used in the present analysis.

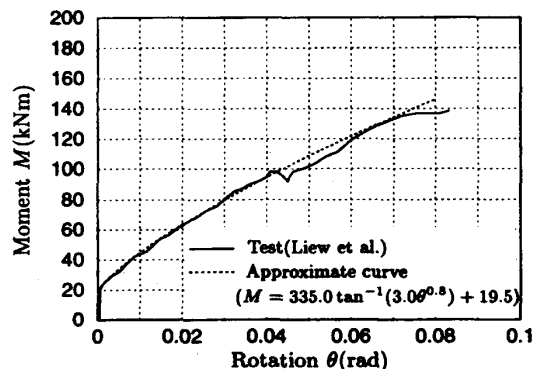Fig. 11 Semi-rigid rectangular frame SRF1 (Liew at el.
1997)

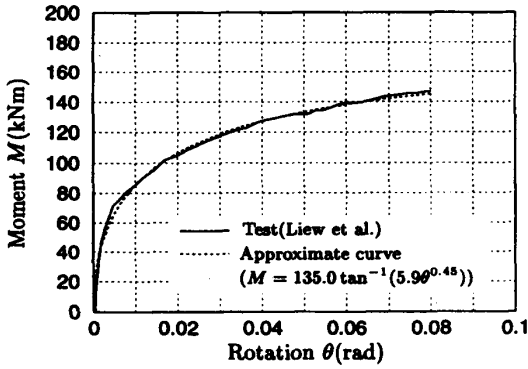Fig. 12 Moment-rotation curve for beam-column joint

Fig. 13 Moment-rotation curve for column base

In the numerical analyses, the elastic shear modulus $G=E/2.6$ and strain hardening modulus $H=E/100$ were assumed. The beam was divided into three elements of equal length, while the column was divided into four elements by the nodes at points 1/10, 1/2, and 9/10 of the column length.

In Fig.14, the horizontal load-lateral displacement curves of the SRF1 frame are compared with the analytical results from the present method. Although the present method underestimates the both experimental and numerical results by Liew et al., the figure shows a reliability of the present method for semi-rigid frames.
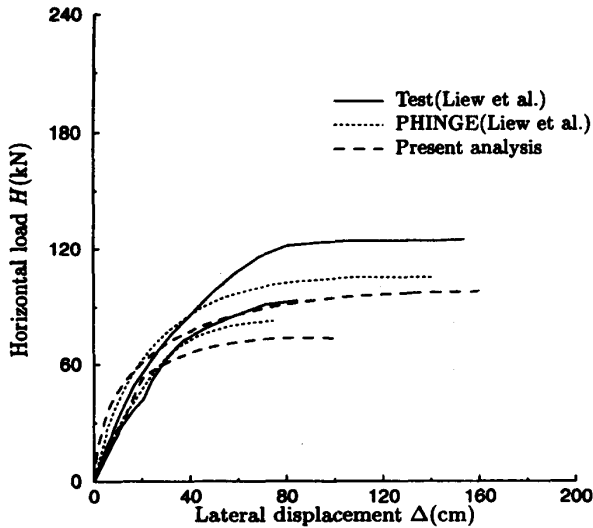

Fig. 14 Comparison of load-displacement curves for SRF1a and SRF1b frames

7.4 Hexagonal Frame with Semi-rigid Joints

(a)Elastic analysis

The hexagonal frame shown in Fig. 15 has been analyzed by many researchers to check the accuracy of the numerical method for analyzing the elastic large deformation behavior of space frames. The properties of the member are as follows: Young's modulus E=3.032 GPa(439.8 ksi), shear

modulus G=1.096GPa(159.0 ksi), cross sectional area A=3.187cm² (0.494in²), torsional constant J=1.378cm⁴ (0.0331in⁴), and moments of inertia $I_y = I_z$ =0.832cm⁴ (0.02in²). In the present analysis, each member was divided into four elements of equal length.
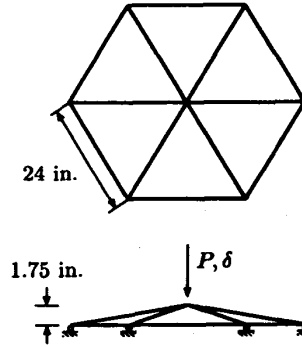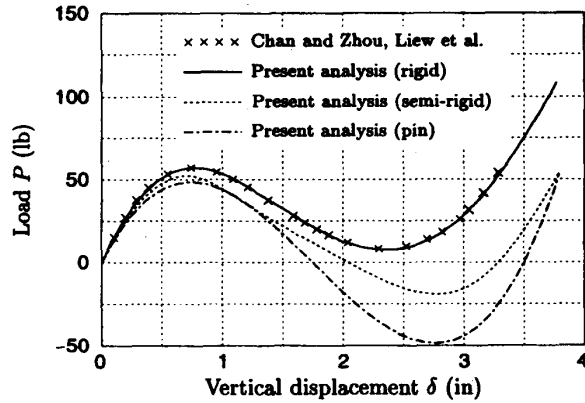

Fig. 15 Hexagonal frame

Fig. 16 Load-vertical displacement curves of hexagonal frame

Figure 16 compares the load-displacement curve for the rigid frame with those obtained by Chan and Zhou (1994) and Liew et al. (1999). The curve obtained by the present method agrees closely with other results.

The dotted line and the dot-dashed line are the load-displacement curves for the cases in which both ends of six roof members have semi-rigid joints and pin joints, respectively. The compliances of the semi-rigid joints were assumed as 0 for axial force, shear force, and torsional moment, and $L/(2EI_y)$, $L/(2EI_z)$ for bending moments where L is the member length.For the pin joints, the same assumption was employed except that $L/(10^8 EI_y)$, and $L/(10^8 EI_z)$ were used as the compliance for bending moments. The dot-dashed line, which passes through points (1.75,0) and (3.5,0), shows the adequacy of the method for the analysis of a pin-connected frame.

(b)Elastoplastic analysis

The results of elastoplastic analyses of the same hexagonal

frame with member properties different from the above example are given in Fig. 17. The member was assumed to be a steel pipe with a circular section having cross sectional area A=3.187cm^2. The member properties are as follows: diameter D=4.674cm, thickness t=0.228cm, Young's modulus E=210.0GPa, shear modulus G=80.77GPa, yield stress σ_y =300.0MPa, and strain hardening modulus H=E/100. Each member was modeled with four equal-length elements. The dotted line and the dot-dashed line in the figure indicate the results for the semi-rigid and the pin-connected frames. The pin-connected frame did not yield. The result for the rigid frame shows that the load after the frame yielded does not vary acutely.
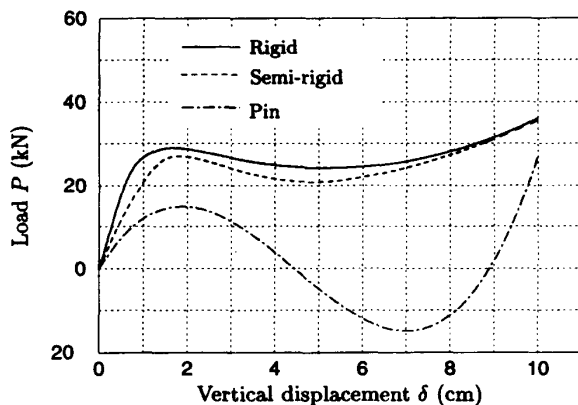

Fig. 17 Load-vertical displacement curves of the steel pipe hexagonnal frame

8 CONCLUSION

An advanced plastic hinge method for accurate analysis of elastoplastic large deformation of three-dimensional steel frames with semi-rigid joints was presented. The effect of shear stress due to St. Venant torsion on the plastic behavior of a member with a closed section is considered using the von Mises yield criterion, the associated flow rule, and Ziegler's hardening rule. The method can be used for the analyses of frames that have open-section members, which cause section warping. It was shown that the use of the 'modified incremental stiffness method' (Stricklin 1971; Washizu 1975) and the updated Lagrangian formulation, together with a precise estimation of the plastic deformation of an element, can increase the accuracy of plastic hinge method. The method does not require a database of the yield surfaces of cross sections and can be introduced in an existing FEM code. The adequacy of the method was verified by comparing the results with the author's experimental results. The accuracy and efficiency of the method were examined through the use of several examples. The results of those examinations demonstrated that an approximation of four elements for a member considering the method's assumptions gives excellent results for the 3D analysis of semi-rigid and pin-connected frames as well as for rigid frames.

REFERENCES

1) Al-Bermani, F. G. A., Kitipornchai, S. (1990). "Elasto-plastic large deformation analysis of thin-walled structures." *Engrg. Struct.*, 12, 28-36.

2) Al-Bermani, F. G. A., and Kitipornchai, S. (1992) "Elastoplastic nonlinear analysis of flexibly jointed space frames." *J. Struct. Engrg.*, ASCE, 118(1), 108-127.

3) Armen, H., Isakson, G., Pifko, A. (1970). "Discrete element method for the plastic analysis of structures subjected to cyclic loading." *Int. J. Numer. Methods in Engrg.*, 2, 189-206.

4) Chan, S. L., Zhou, Z. H., (1994). "Pointwise equilibrating polynomial element for nonlinear analysis of frames." *J. Struct. Engrg.*, ASCE, 120(6), 1703-1717.

5) Chen, W. F., Atsuta, T. (1977). *Theory of Beam-Columns*, Vol. 2, McGraw-Hill, New York.

6) Crisfield, M. A. (1997). *Non-linear Finite Element Analysis of Solids and Structures*, Vol. 2, Advanced Topics, John Wiley & Sons.

7) Hall, J. F., Challa, V. R. M. (1995). "Beam-column modeling." *J. Engrg. Mech.*, ASCE, 121(12), 1284-1291.

8) Harrison, H. B. (1964). "The application of the principles of plastic analysis to three-dimensional steel structures." Ph.D. thesis, Dept. of Civ. Engng., University of Sydney, Australia.

9) Izzuddin, B. A., Lloyd Smith, D. (1996). "Large-displacement analysis of elastoplastic thin-walled frames. I: Formulation and implementation." *J. Struct. Engrg.*, ASCE, 122(8), 905-925.

10) King, W.S., Chen, W. F. (1994). "Practical second-order inelastic analysis of semirigid frames." *J. Struct. Engrg.*, ASCE, 120(7), 2156-2175.

11) Kouhia, R., and Tuomala, M. (1993). "Static and Dynamic analysis of space frames using Timoshenko type elements ." *Int. J. Numer. Methods in Engrg.*, 36, 1189-1221.

12) Liew, J. Y. R., Chen, H., and Shanmugam, N. E. (1999). "Stability functions for second-order inelastic analysis of space frames." *Light-Weight Steel and Aluminium Structures*, Elsevier, 19-26.

13) Liew, J. Y. R., White, D. W., and Chen, W. F. (1993). "Second-order refined plastic-hinge analysis for frame design: Part I." *J. Struct. Engrg.*, ASCE, 119(11), 3196-3216.

14) Lui, E. M., and Chen, W. F. (1986). "Analysis and behaviour of flexibly-jointed frames." *Eng. Struct.*, 8(2), 107-118.

15) Lui, E. M., and Chen, W. F. (1987). "Steel frame analysis with flexible joints." *J. Const. Steel Res.*, 8, 161-202.

16) Ramm, E. (1982). "The Riks/Wempner approach - an extension of the displacement control method in nonlinear analysis." Recent Advances in Nonlinear Computational Mechanics., Pineridge Press, 63-86.

17) Shakourzadeh H, Guo, Y. Q., and Batoz J. L., (1999) "Modeling of connection in the analysis of thin-walled space frames." *Comput. Struct.*, 71, 423-433.

18) Shugyo, M., Li, J.P., and Oka, N. (1995). "Inelastic stability of linearly tapered box columns under biaxial bending and torsion." *Report of the Faculty of Engrg, Nagasaki Univ.*, 25(45), 143-149.

19) Shugyo, M., Oka, N., and Li, J.P. (1996). "Inelastic nonlinear analysis of steel space frames with flexible joints."*J. Struct. Constr. Eng.*, Architectural Institute of Japan, 480, 89-94 (in Japanese).

20) Stricklin, J. A., Haisler W. E., and von Riesemann, W. A. (1971). "Geometrically Nonlinear Structural Analysis by Direct Stiffness Method." *J. Struct. Div.*, ASCE, 97(9), 2299-2314.

21) Teh, L. H., Clarke, M. J. (1999). "Plastic-zone analysis of 3D steel frames using beam elements." *J. Struct. Engrg.*, ASCE, 125(11), 1328-1337.

22) Washizu, K. (1975). *Variational methods in elasticity and plasticity*, 2nd ed., Pergamon Press.